Available online at www.sciencedirect.com
SCIENCE DIRECT
Carbohydrate Polymers 60 (2005) 399–409
Carbohydrate Polymers
www.elsevier.com/locate/carbpol

Intermolecular interaction and properties of cross-linked materials from poly(ester-urethane) and nitrochitosan

Ming Zeng[a], Lina Zhang[a,*], John F. Kennedy[b,c]

[a]*Department of Chemistry, Wuhan University, Wuhan 430072, People's Republic of China*
[b]*Birmingham Carbohydrate and Protein Technology Group, School of Chemical Sciences, The University of Birmingham, Birmingham BI5 2TT, UK*
[c]*Chembiotech Laboratories, University of Birmingham Research Park, Vincent Drive, Birmingham BI5 2SQ, UK*

Received 28 February 2004; revised 5 February 2005; accepted 7 February 2005
Available online 7 April 2005

Abstract

Two series of semi-interpenetrating polymer network (semi-IPN) films, coded as PUNT and PUN, have been prepared from amorphous nitrochitosan (NCH) and semicrystalline poly(ester-urethane) (PU) cross-linked to the hydroxy groups of tris(hydroxymethyl)propane (TMP) and NCO groups of PU prepolymer, respectively, by a casting method. The effects of different cross-linking methods and NCH content on the crystallization and hydrogen bonding strengths of the films were studied by attenuated total reflection Fourier transform infrared spectroscopy (ATR-FTIR) with the curve fitting method and wide angle X-ray diffraction (WAXD). The miscibility and mechanical properties of the films were measured by dynamic mechanical analysis (DMA), scanning electron microscopy (SEM), density measurement, thermogravimetric analysis (TGA), tensile testing and solvent swelling testing. The results revealed that the degree of crystalline for the semi-IPN films was lower than that of PU, because of the addition of amorphous NCH to destroy the original ordered structure in the PU film. Moreover, the crystal domain formation for the PUNT films cross-linked with TMP can be more easily interrupted than to other self-crosslinked PUN films without TMP, resulting in a new disordered hydrogen bonded band in ATR-FTIR spectra. The PUNT films exhibited better miscibility as well as higher density, thermal stability, tensile strength and water resistance than the PUN films, suggesting an effective interpenetration and dense network structure. The differences between the two series of the films can be attributed to a relatively dense cross-linking network and strong intermolecular hydrogen bonding occurred between NCH and PU in the PUNT films as a result of the reaction cross-linked with TMP. It is noted that with an increase of NCH from 5 to 30% w/w, the thermal stability, tensile strength and water resistance of the PUNT films increased.

Keywords: Interpenetrating polymer networks; Cross-linking; Crystallization; Nitrochitosan

1. Introduction

Polyurethanes (PU) are a versatile class of man-made polymers used in a wide variety of products in the medical, automotive and industrial fields (Brinkman & Vandevoorde, 1998; Duecoffre, Diener, Flosbach, & Schubert, 1998), and have been found to be susceptible to biodegradation by microorganisms (Howard, 2002). The composite materials prepared from PU and natural polymers possess potential application where biodegradation is very important. After cellulose, chitin is the second most abundant natural polymer on earth. The principle derivative of chitin, chitosan, is obtained by *N*-deacetylation (Muzzarelli, 1977). Chitin and chitosan have been widely used in the fields of medicine, pharmaceutics, paper production, textiles, metal chelation, food additives, antimicrobial agents, adhesives, and other industrial applications (Migashita, Kobayashi, & Nishio, 1997; Welsh, Schauer, Qadri, & Price, 2000). It is worth noting that chitosan is from annually renewable resources, and has a peculiar molecular structure quite different from those of synthetic polymers (Kurita, 2001). However, the use of chitosan as a material has been challenged by some limitations, because of the low solubility in most organic solvents, low moisture resistance, high brittleness and incompatibility with some hydrophobic polymers.

* Corresponding author. Tel.: +86 27 87219274; fax: +86 27 68756661.
E-mail address: lnzhang@public.wh.hb.cn (L. Zhang).

0144-8617/$ - see front matter © 2005 Elsevier Ltd. All rights reserved.
doi:10.1016/j.carbpol.2005.02.002

Polymer blends continue to be a subject of intensive investigations because of the simplicity and effectiveness of mixing two different polymers to obtain new materials from both academic and industrial views (Sperling, 1981; Thomas & Sperling, 1979). Some blend techniques provide novel ways for modification and exploitation of natural polymers (Gao & Zhang, 2001; Lu & Zhang, 2002; Zeng, Zhang, Wang, & Zhu, 2003; Zeng, Zhang, & Zhou, 2004; Zhang & Zhou, 1999). In our laboratory, semi-interpenetrating polymer network (semi-IPN) materials derived from castor oil-based polyurethane and derivatives of natural polymers such as nitrokonjac glucomannan (Gao & Zhang, 2001), benzyl konjac glucomannan (Lu & Zhang, 2002), and nitrocellulose (Zhang & Zhou, 1999) have been synthesized, and coated onto regenerated cellulose (RC) films to improve mechanical properties and water resistance. Interestingly, the RC films coated with the semi-IPN coatings can be degraded by microorganisms in soil, accompanied by the production of CO_2, H_2O, glucose and aromatic ether cleaved from cellulose and PU (Zhang, Zhou, Huang, & Gong, 1999). Therefore, the semi-IPN from PU and natural polymers provide potential materials that are important for a sustainable development and environmental conservation.

A basic understanding of structure and crystallization behavior of materials is essential for their application. However, the crystalline behavior of polymer blends containing crystalline or semicrystalline polymers are less well understood because of their inherent complexities (Kuo, Chan, & Chang, 2003; McKiernan, Heintz, Hsu, Atkins, Penelle, & Gido, 2002). Our research interest lies on blending of modified chitosan and semicrystalline polyester PU to create a biodegradable material with good mechanical properties and miscibility. It is well known that the cross-linking networks strongly influence properties of the semi-IPN materials. Therefore, we attempted to prepare PU polymer network cross-linked with hydroxyl groups of tris(hydroxymethyl)propane (TMP) and NCO groups of PU prepolymer by using different cross-linking methods. The objective of this study was to explore the effects of the cross-linking networks and NCH content on the crystallization, miscibility and properties of the blend films. The hydrogen bonding strengths and intermolecular interaction were studied by attenuated total reflection Fourier transform infrared spectroscopy, wide angle X-ray diffraction, scanning electron microscopy, dynamic mechanical analysis and density measurement.

2. Experimental

2.1. Synthesis of nitrochitosan

Chitosan was supplied by Yuhuan Sea Biochemical Co., Zhejiang, China. Its weight-average molecular weight (M_w) and degree of deacetylation were 1.5×10^5 and 90%, respectively. The nitrochitosan (NCH) was prepared by adding chitosan (1 g) slowly into nitric acid (150 mL), which was cooled by using an ice/salt bath, then 100 mL of acetic anhydride was introduced in droplet under vigorous stirring. Four hours later, the mixture was poured into ice water to end the reaction. The precipitate was collected and washed thoroughly with distilled water and then with ethanol. It was purified by redissolving in acetone, and filtered to remove the insoluble part. After evaporating the solvent, the product was vacuum-dried at room temperature for 10 h to obtain a white powder. Its M_w was measured to be ca. 8.1×10^4 by a multiangle laser photometer (MALLS, DAWN-DSP, Wyatt Technology Co.) combined with a P 100 pump (Thermo Separation Products, San Jose, Japan), equipped with a TSK-GEL G4000 HHR column (7.8×300 mm) at a flow rate of 1.0 mL/min with tetrahydrofuran (THF; distilled and dried over sodium sulphate before use) as eluent at 25 °C. The Fourier transform infrared spectrum of the product showed the same result as we reported before, suggesting that we had successfully prepared the nitrochitosan (Liu & Zhang, 2001).

2.2. Preparation of poly(ester-urethane) prepolymer

The value of [NCO]/[OH] was predetermined theoretically to be 1. Poly(ethylene glycol adipate) (PEGA; 66.5 g; $M_n=2499$; Tiangou Polyurethane Factory, Jiangsu, China) was vacuum-dried for 5 h at 110 °C before use. Its acid value (mg KOH/g) and OH value (mg KOH/g) were 0.20 and 44.7, respectively. Commercial 2,4-toluene-diisocyanate (TDI; 11.6 g; Shanghai Chemical Co., Shanghai, China; redistilled under reduced pressure to be dehydrated before use) was dropped into the PEGA melt at 85 °C for 2 h to obtain the PU prepolymer. Then, 2,2-bis(hydroxymethyl) propionic acid (35 g; Chengdu Polyurethane Factory, Sichuan, China; vacuum-dried for 2 h at 110 °C before use) were added into the prepolymer to continue the chain-extending reaction for another 1 h until the NCO groups content reached a given value, determined by dibutylamine back titration (Hepburn, 1982). After the mixture had then cooled to 40 °C, THF (90 g) was added to adjust the solid content of the resulting mixture to 40 wt%.

2.3. Preparation of PU/NCH films

1,1,1-Tris(hydroxymethyl)propane (TMP; Shanghai Chemical Co., Shanghai, China; dried to moisture content less than 0.1 wt%) was used as the cross-linker of polyester PU prepolymer. The mixtures of PU prepolymer and the predetermined amount of NCH with or without TMP (2.5 wt% of the solid content of PU prepolymer) were mechanically stirred in THF for 3 h to obtain transparent solutions. The solid contents of the mixtures were adjusted to be 15 wt% by diluting with THF. The clear mixture solutions were cast on glass plates and cured at room temperature for 24 h. To ensure complete elimination of

the solvent, the blend film was then dried at 60 °C for 2 h. The thickness of the film was measured to be ca. 380 μm. By altering the weight percentage content of NCH (w_{NCH}) in the blend films to 5,10, 20 and 30 wt%, two series of the films cross-linked with and without TMP were prepared, and coded as PUNT5, PUNT10, PUNT20, PUNT30, and PUN5, PUN10, PUN20 and PUN30, respectively. The pure PU films self-crosslinked without TMP, and cross-linked with TMP, were coded as PU and PUT, respectively. The film from pure NCH could not be obtained by the casting method because of its brittleness. The samples were kept at room temperature for at least two weeks before the measurements were conducted.

2.4. Characterization

Attenuated total reflection Fourier transform infrared (ATR-FTIR) spectroscopy was carried out on a Thermo Nicolet 670 spectrometer (USA). Spectra in the range from 4000 to 500 cm^{-1} were collected over 64 scans with a resolution of 4 cm^{-1}. The measurements were made at room temperature, on a diamond using a variable-angle ATR unit at a nominal incident angle of 45°. Optical alignment of the unit was set to achieve maximum throughput of the infrared beam to the detector. Samples were taken at random from the flat films. The curve-fitting simulations of ATR-FTIR spectra were performed using a standard Origin 6.0 software program. The bands of γ(NH) and γ(C=O) were deconvoluted, considering peaks as Gaussian. Caution was taken in not overestimating the number of peaks since the additional degree of freedom afforded by too many peaks would always provide a better fit.

Wide-angle X-ray diffraction (WAXD) patterns were recorded on an X-ray diffractometer (XRD-6000, Shimadzu, Japan), by using Cu Kα radiation ($\lambda = 15.405$) at 40 kV and 30 mA with a scan rate of 4°/min. The diffraction angle ranged from 4 to 35°. Dynamic mechanical analysis (DMA) was carried out with a dynamic mechanical thermal analyzer (DMTA-V, Rheometric Scientific Co., USA) at 1 Hz and a heating rate of 5 °C/min in the temperature range from −50 to 200 °C. Specimens with a typical size of ca. 10×10 mm (length×width) were used here.

Scanning electron microscopy (SEM) images of the films were taken with a microscope (X-650, Hitachi, Japan). The films were frozen in liquid nitrogen and snapped immediately, and then vacuum-dried. The surface and cross-section of the films were sputtered with gold, and then observed and photographed.

The density (ρ) of the films were measured at 30 °C by determining the weight of a volume-calibrated psychomotor filled with a mixture of sodium chloride aqueous solution and distilled water, in which the samples achieved floatation level. The density of the liquid mixture equals the density of the samples. Three parallel measurements were carried out for every sample.

Thermogravimetric analysis (TGA) of the films with 1 mm width and 1 mm length were carried out with a thermobalance (SETSYS-16, Setaram, France) under a nitrogen atmosphere from 25 to 500 °C, at a heating rate of 10 °C/min. Tensile strength and elongation at break of the films were measured on a tensile tester (CMT-6503, Shenzhen SANS Test Machine Co. Ltd, China) according to the ISO 6239-1986 standard with a tensile rate of 5 mm/min. The size of the films was 70 mm length, 10 mm width, with 50 mm distance between two clamps. Five parallel measurements were carried out for each sample.

Water absorption of the films was determined by immersing the cut films in water at 37 °C. The films, 1 mm thick, were cut into circular disks by using a sharp-edged stainless steel die with an inner diameter of 20 mm. The samples were weighed every 10 min until they attained the maximum water content. Three parallel measurements were carried out for each sample. The water absorption (WS) of the films was calculated by

$$WS = [(w_s - w_d)/w_d] \times 100\% \quad (1)$$

where w_s is the weight of swollen film, w_d is the weight of the dry film.

3. Results and discussion

3.1. Structure and interaction of blends

ATR-FTIR study on the NH and C=O regions provides a powerful method to evaluate the confirmation change of urethane polymers (Chen, Yu, & Chen, 2001; Luo, Wang, & Ying, 1996; Yen & Hong, 1997; Yen, Lin, & Hong, 1999). In this investigation, ATR-FTIR was used to study the effect of different cross-linking networks and the amounts of NCH on polyester crystallinity as soft segments of PU, on the basis of the peak shifts and intensity changes. In the typical infrared spectra (4000–500 cm^{-1}) of the PU, PUT, PUN10 and PUNT10 films (Fig. 1), curve fitting of two especial regions are of main interest: the C=O stretching vibration from 1600 to 1800 cm^{-1} and the NH stretching vibration from 3150 to 3550 cm^{-1} (Fig. 2). Five Gaussian bands between 1600 and 1800 cm^{-1} corresponding to free, disordered hydrogen bonded and ordered hydrogen bonded urethane carbonyl groups, free and hydrogen bonded ester carbonyl groups were employed in the fitting procedure. The frequency (γ) and the width at half-height ($W_{1/2}$) related to the strength of hydrogen bonding are listed in Table 1. The results obtained by curve-fitting procedures represent a quantitative but relative measurement of the amount of the species. In these simulations, the values of the absorptive coefficients of the different bands were not considered. The frequency of the free urethane and ester carbonyl stretching vibrations remained essentially constant for all films, with values 1727 ± 1 cm^{-1} ($W_{1/2} = 12 \pm 2$ cm^{-1}) and

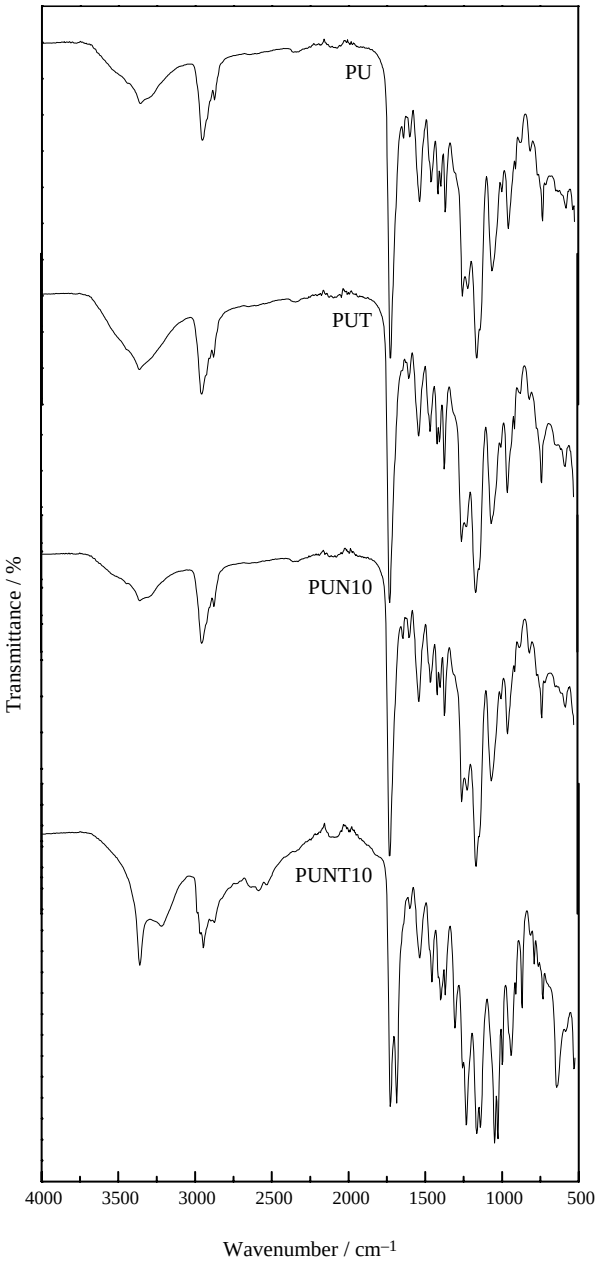

Fig. 1. ATR-FTIR spectra of the films PU, PUT, PUN10 and PUNT10.

$1725 \pm 2\ cm^{-1}$ ($W_{1/2} = 25 \pm 1\ cm^{-1}$), respectively. The C=O stretching band at around $1642\ cm^{-1}$ was resulted from the hydrogen bonded C=O formed from the NH of urethane and C=O of polyester.

For the PUN films, the band at $1705 \pm 2\ cm^{-1}$ was attributed to the ordered hydrogen bonded urethane carbonyl groups. Compared with the band of PU, the frequency of the band shifted to higher values with an increase of NCH content in the blend films, indicating that the strength of the hydrogen bonds became weaker. Furthermore, with an increase of NCH content in the blend films, the width at half-height of the band increased from 47.29 to $67.17\ cm^{-1}$, reflecting intermolecular

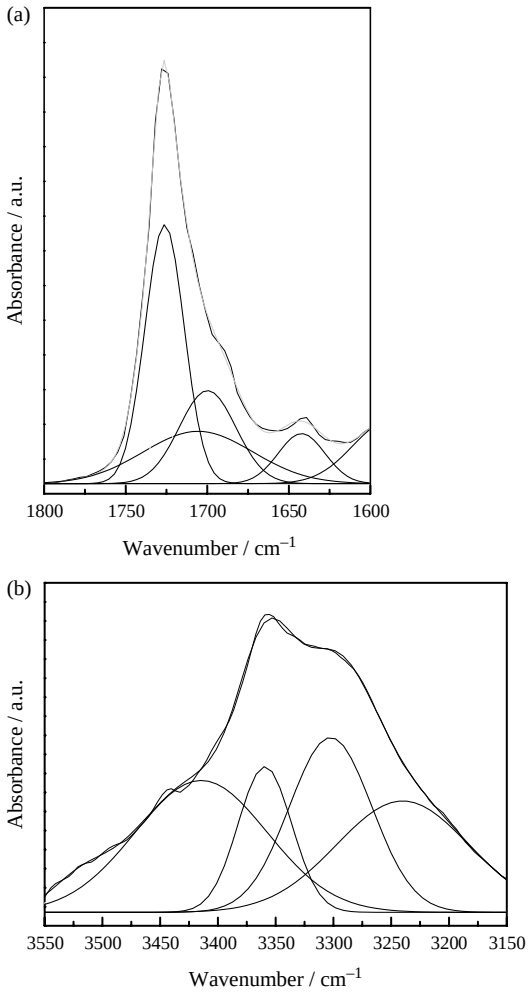

Fig. 2. Experimental (—) and simulated (– · –) ATR-FTIR spectra in the C=O (a) and NH (b) stretching regions of PUN10 film.

interactions between NCH and PU; this resulted in an increase of the degree of disorder in PU. However, the frequency of ordered hydrogen bonded urethane carbonyl band shifted to lower values with an increase of NCH in the PUNT films, indicating that the strength of the hydrogen bonds between PU and NCH became stronger. Moreover, with an increase of NCH, the band at $1710\ cm^{-1}$ corresponding to the disordered hydrogen bonded urethane carbonyl groups appeared, suggesting that original inter- and intra-molecular hydrogen bonds in the PU networks were destroyed as a result of the interpenetrating and entanglements between NCH and PU.

The NH stretching vibration yields structural information complementary to the C=O stretching vibration. Deconvolution of the NH stretching region was performed and Gaussian functions were used. A flat baseline was chosen from 3150 to $3550\ cm^{-1}$. The limits of the curve fitting were set between 3200 and $3500\ cm^{-1}$. Considering the polyurethane literature, the peak centered at $3400\ cm^{-1}$ corresponds to the free NH stretching mode, and two bands are assigned to NH bonded to carbonyl groups at $3359\ cm^{-1}$ and

Table 1
Frequency (γ) and width at half-height ($W_{1/2}$) of the five components of the C=O stretching band

Samples	Urethane						Ester			
	Free		Hydrogen bonded				Free		Hydrogen bonded	
	γ	$W_{1/2}$	Disordered		Ordered		γ	$W_{1/2}$	γ	$W_{1/2}$
			γ	$W_{1/2}$	γ	$W_{1/2}$				
PU	1727	10.58			1703	47.29	1723	24.88	1642	27.09
PUN5	1727	10.77			1707	47.22	1724	26.57	1641	38.28
PUN10	1727	10.91			1705	47.12	1725	24.67	1641	30.95
PUN20	1728	10.54			1705	67.17	1726	24.04	1642	28.66
PUN30	1728	10.67			1705	64.45	1726	24.21	1642	30.01
PUT	1726	12.74			1705	47.38	1724	25.57	1642	42.60
PUNT5	1727	10.77			1705	48.32	1724	24.91	1641	29.94
PUNT10	1728	14.62	1710	45.68	1685	47.77			1647	33.99
PUNT20	1728	12.15	1710	47.27	1683	34.99			1643	36.34
PUNT30	1728	12.21	1710	48.37	1683	44.72			1645	32.02

NH bonded to the ether oxygen at around 3304 cm^{-1}. The last band of the curve fitting is centered at 3245 cm^{-1}. The NH stretchings generally have a strong dependence of their extinction coefficients upon absorption frequencies, and this results in the conformational insensitivity of the NH scarce data on extinction coefficients and the uncertainty on the peak areas. Therefore, no data on the peak areas are listed in Table 2.

In the simulation and deconvolution of the bands for the blend films with different compositions (Table 2), the frequency of hydrogen bonded ether oxygen in the PUN films shifted to the higher values and the bandwidths increased slightly with an increase of NCH content. This implies that intermolecular interaction between the components resulted in a decrease of the degree of order in the PUN films. No contribution from the free NH group was detected, and the bandwidths of the deconvoluted components changed significantly for the PUNT films. The width at half-height of the band corresponding to NH hydrogen bonded to nitryl groups increased from 65.95 to 165.9 cm^{-1}, and carbonyl groups decreased from 53.18 to 27.28 cm^{-1} with an increase of the NCH content of the PUNT films. This can be interpreted in terms of a broadening of the distribution of hydrogen-bonded distances and geometries when the NCH content increased, enhancing the miscibility between the components.

Changes in the frequency and intensity of C=O and NH absorption bands are correlated to structural alteration. The results obtained gave evidence that as NCH content for the PUN films further increased, the band maximum shifted to the higher frequencies, corresponding to a reduction in the average strength of the hydrogen bonds between NCH and PU, indicating the formation of a less ordered structure. The results also confirmed that there are stronger interactions between PU and NCH for the PUNT films to decrease the degree of crystallinity of PU, leading to the broadening of bandwidths and appearance of the new disordered hydrogen bonded band. Therefore, stronger intermolecular interactions between PU and NCH occurred more easily in the semi-IPN system cross-linked with TMP than in that self-crosslinked with the NCO groups of the PU prepolymer.

The WAXD patterns of the PU films cross-linked with TMP and self-crosslinked (Fig. 3) all exhibited three peaks at $2\theta = 18.32$ (4.84 Å), 22.20 (4.00 Å) and 24.50° (3.63 Å), $2\theta = 18.12$ (4.89 Å), 22.02 (4.03 Å) and 24.58° (3.62 Å), respectively, which attributed to the order arrangement of

Table 2
Frequency (γ) and width at half-height ($W_{1/2}$) of the four components of the NH stretching band

Samples	Free		Hydrogen bonded				Overtone	
	γ	$W_{1/2}$	NH···C=O		NH···O		γ	$W_{1/2}$
			γ	$W_{1/2}$	γ	$W_{1/2}$		
PU	3400	114.3	3359	44.02	3301	67.98	3243	103.5
PUN5	3449	134.5	3350	67.43	3290	66.11	3230	102.5
PUN10	3414	114.3	3359	46.44	3302	71.31	3240	114.6
PUN20	3454	142.3	3362	39.00	3304	67.89	3265	165.7
PUN30	3451	139.1	3360	40.13	3304	70.31	3255	174.2
PUT	3416	134.1	3359	53.18	3300	74.13	3228	102.2
PUNT5	3405	158.4	3357	48.79	3296	65.95	3228	83.86
PUNT10			3360	27.28	3341	144.5	3197	120.9
PUNT20			3361	28.84	3343	165.9	3195	118.7
PUNT30			3360	28.37	3343	158.1	3195	121.4

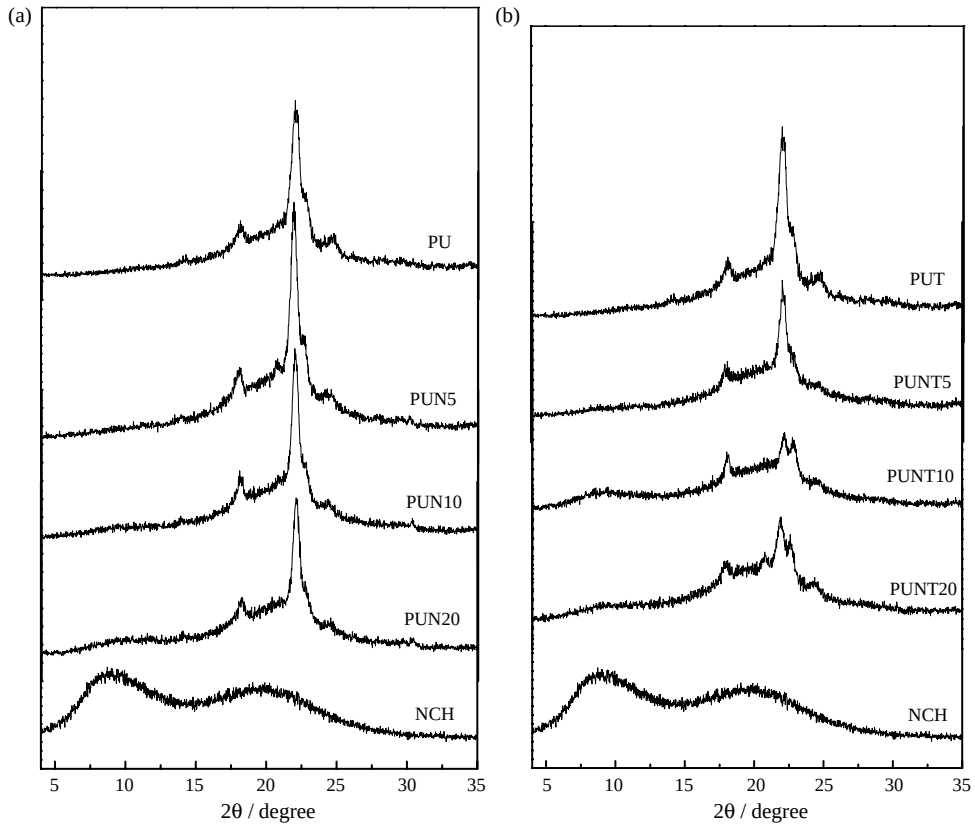

Fig. 3. WAXD spectra of PUN (a) and PUNT (b) films.

the PU polyester soft segment (Chen et al., 2001). Two broad reflections centered at 9.00 (9.82 Å) and 20.22° (4.39 Å) for NCH powder, indicating the amorphous nature. The WAXD patterns of the films PUN and PUNT are also shown in Fig. 3. All of the diffraction profiles of the PUN films exhibited the presence of two sharp peaks at $2\theta = 22.02$ and 24.58°. The intensities of the peaks were almost the same as, or slightly lower, than the pure PU film, suggesting that the ordered structure hardly changed, which supports the results from the infrared analysis for PUN films.

When NCH content increased from 5 to 10 wt%, a sharp crystalline diffraction peaks emerged in the high-angle region ($2\theta = 24.47°$) for the PUNT films, corresponding to an intermolecular distance of 3.64 Å. Concurrently, the diffraction peak in the low-angle region ($2\theta = 8.34°$, 10.59 Å) appears, indicating an enhancement of the long-range order (Queiroz, de Pinho, & Dias, 2003). The strong intermolecular interactions between NCH and PU for the PUNT films are supposed to retard the arrangement of the molecular chains in a regular manner for polyester PU. Generally, when the crystalline component and the amorphous component in a composite material are in good miscibility, its degree of crystalline is lower than that of the individual crystalline component on its own. Therefore, the decrease in the degree of crystalline of the PUNT films suggests a relatively strong intermolecular interaction between NCH and PU.

The decrease in the degree of crystallinity of PU in the blends was found by using ATR-FTIR and WAXD. The suppression of PU crystallization found in the blends with NCH might be due to at least two factors (Ikejima & Inoue, 2000). One is the formation of the intermolecular hydrogen bond between NCH and polyester PU networks. Another is the rigid environment that arises from inflexible polysaccharide molecules. In addition, the degree of crystallinity of PUNT films was obviously lower than that of PUN films. This further supports the conclusion from ATR-FTIR that NCH more easily interrupts the crystal domain formation for the PUNT films.

3.2. Miscibility and interaction of blends

Usually, mechanical loss factor (tan δ) peak in the DMA thermogram, the α-relaxation, reflects the glass transition, and may be analyzed to provide information about the motion of molecules. If the two starting materials had phase separation and prevented interaction, there are two T_g peaks corresponding to two components for the blends. Fig. 4(a) depicts tan δ spectra of the self-crosslinked PUN films. T_g of NCH was measured to be around 150 °C, and PU has a T_g of 68 °C. There are double peaks of T_g in the DMA

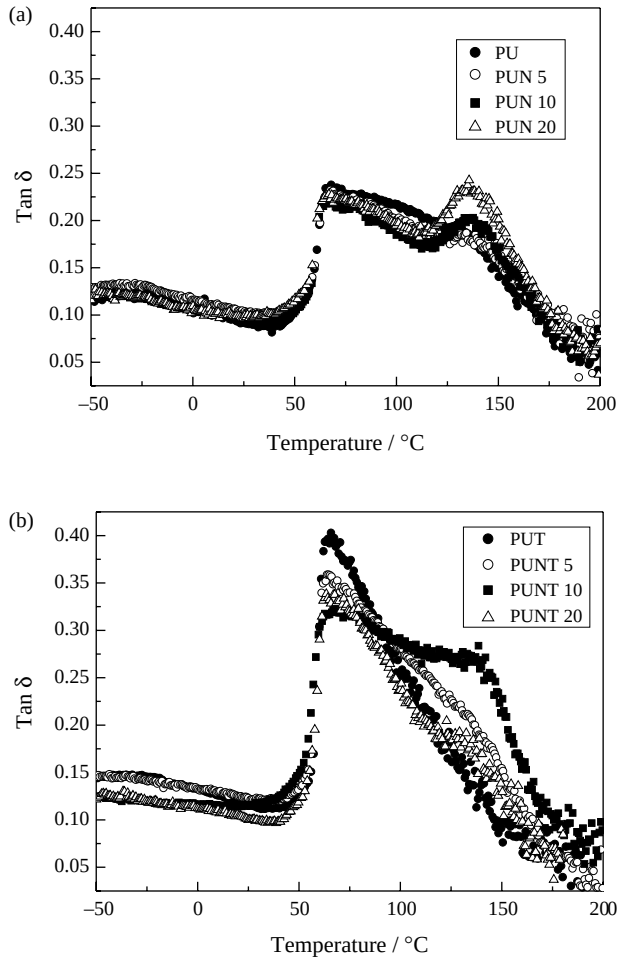

Fig. 4. Tan δ as a function of temperature for PUN (a) and PUNT (b) films.

thermogram for the PUN films, indicating a certain degree of micro-phase separation between NCH and PU. Furthermore, the height and width of the α-relaxation peak can be used to analyze the molecular motion of cross-linking polymers. The intensity of the T_g peak of PU for the PUN films hardly changed with an increase of NCH, indicating that they have similar PU network structure. Fig. 4(b) shows the tan δ spectra of PUNT films. The T_g values of PU for PUNT films with NCH added were determined to be 65 °C, which was lower than that of the PUN films. The reduction of T_g suggests the micro-phase separation between soft and hard segments of PU (Gao & Zhang, 2001), as a result of the addition of cross-linker TMP. As the NCH content increased to 10 wt%, the DMA thermogram showed a broad peak with main and shoulder peaks, indicating multi-molecular motion of the polymer material. As the NCH content further increased to 20 wt%, the twin maxima in the tan δ thermogram gradually merge to produce a single maximum. The difference in the DMA thermograms between the films PUNT and PUN confirmed that better miscibility occurs between the components of the PUNT films than between those of PUN films. In addition, the intensities of tan δ peak of PU in the PUNT films were higher than that in the PUN films. However, the intensities of tan δ peaks related to PU in the PUNT films decreased with an increase of NCH content, owing to the improvement of cross-linking density (Ishida & Allen, 1998).

SEM observation can give information of the morphological change and miscibility and the SEM images of the surface and cross-section of the films PU and PUN are shown in Fig. 5. The surface morphologies of PUN films were almost the same as that of PU films. The cross-section of the PUN films exhibited heterogeneous morphology with some holes caused by the dispersed NCH particles in the PU cross-linking networks. However, different morphology of the PUNT films was observed (Fig. 6) and no clear domain structure appeared, compared with the micro-domain structure of PUN films, indicating a stronger interaction between components NCH and PU for the PUNT films. When the NCH content increased from 5 to 20 wt% in the PUNT films, the cross-section morphologies became more dense and homogeneous, suggesting the effectiveness of the intermolecular penetration. In view of the SEM analysis of PUN and PUNT films, the relatively strong intermolecular interaction between PU and NCH occurred in the PUNT films to interrupt the crystal domain and form compact cross-linking networks, resulting in a good miscibility between both components.

In a polymer blend where no adhesion between the interface and no molecular mixing occur at the phase boundary, the density of the blend would be expected to follow the rule of mixtures (Lu & Zhang, 2002). As a result, the positive deviation of the densities for IPN material can be attributed to intimate interpenetration and chain packing, leading to reduction of the free volume. As shown in Fig. 7, the PUNT films showed stronger positive density deviations than PUN films when the NCH content was less than 20 wt%, indicating an intimate interpenetration of interchains between PU and NCH in the PUNT films. The difference between two semi-IPN systems can be explained in that the short chain monomer TMP may more readily react with TDI to form a network for the PUNT system which is relatively denser than the PUN system self-crosslinked with the NCO groups of PU prepolymer. When the molecular chain of the PU prepolymer was relatively long, the cross-linking structure formation was relatively difficult. The results of the density measurement supported the conclusion from DMA, namely good miscibility of PUNT films.

3.3. Thermal and mechanical properties of blends

In the thermogravimetric curves of the blends (Fig. 8), a small weight loss at 25–200 °C was assigned to the release of moisture and solvent from the samples. Generally, the thermal degradation of a semi-IPN system in dynamic condition shows three decomposition stages (Cascaval, Rosu, Rosu, & Ciobanu, 2003; Filip, Simionescu, & Macocinschi, 2002). The degradation onset temperature

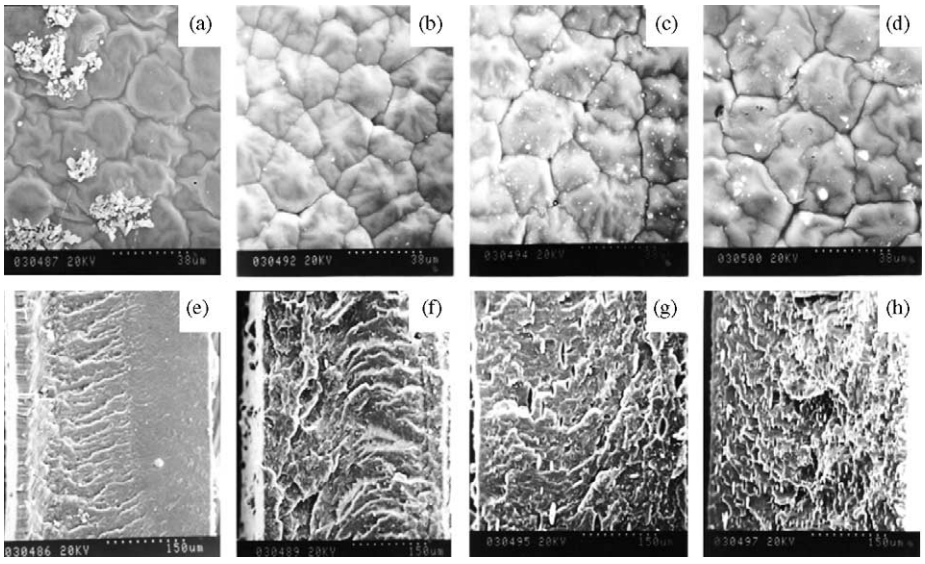

Fig. 5. SEM photographs for films of PU (surface, a; cross-section, e), PUN5 (surface, b; cross-section, f), PUN10 (surface, c; cross-section, g) and PUN20 (surface, d; cross-section, h).

(T_{10}) of the films was around 300 °C (start for the first stage), and an increasing decomposition rate was observed between 350 and 400 °C (the second stage) when the weight losses reached about 60–70 wt%. The third stage of decomposition temperatures were higher than 400 °C, corresponding to the advanced fragmentation of the polymer chain formed in the first and second stages of decomposition, as well as the secondary reactions of dehydrogenation and gasification processes. Almost complete decomposition was observed at 500 °C. Data of the temperature corresponding to 10 (T_{10}), 50 (T_{50}) and 80 wt% (T_{80}) weight loss from the initial weight, as well as temperature taken for the maximum rate of decomposition (T_d) along with initial decomposition (T_i) are summarized in Table 3. The values of T_d for the PUN films were all slightly higher than that of the PU film, suggesting that the addition of NCH enhanced the thermal stability. It was noted that the values of T_{10}, T_{50}, T_m, and T_{80} of PUNT films were all higher than that of the PUT film, implying that an enhancement of thermal stability caused by cross-linking with TMP. The difference of thermal stability between PUNT and PUN films can be attributed to different cross-linked structures.

In the NCH content dependence of the tensile strength (σ_b) and elongation at break (ε_b) for the PUN and PUNT films (Fig. 9), the ε_b values of both IPN systems decreased

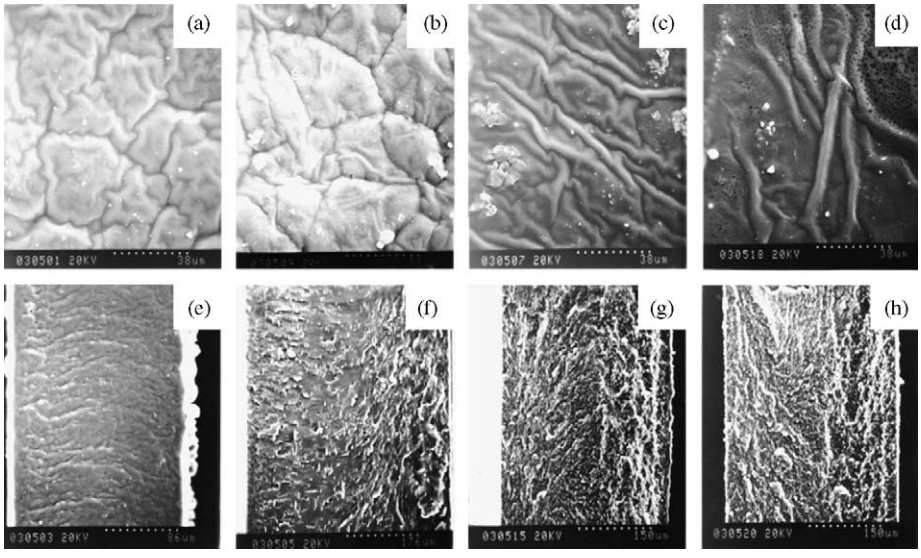

Fig. 6. SEM photographs for the films PUT (surface, a; cross-section, e), PUNT5 (surface, b; cross-section, f), PUNT10 (surface, c; cross-section, g) and PUNT20 (surface, d; cross-section, h).

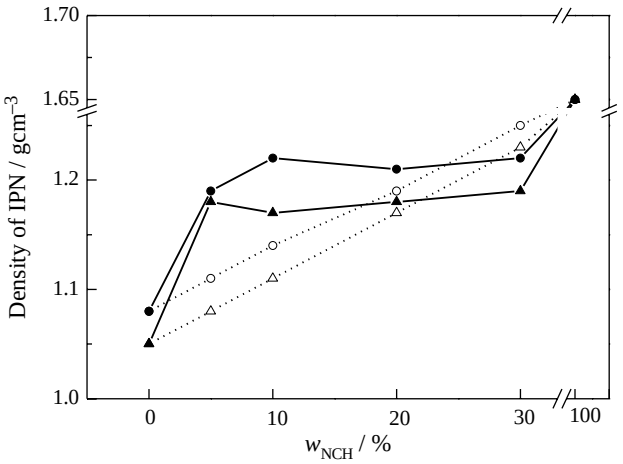

Fig. 7. NCH content (w_{NCH}) dependence of the densities from theoretical values (○) and (△), and experimental values for PUNT (●) and PUN (▲) films, respectively.

with an increase in NCH content. However, the tensile strengths of all the semi-IPN systems increased with an increase of NCH content up to 20 wt% for PUN films and 10 wt% for PUNT films, and then decreased. These results

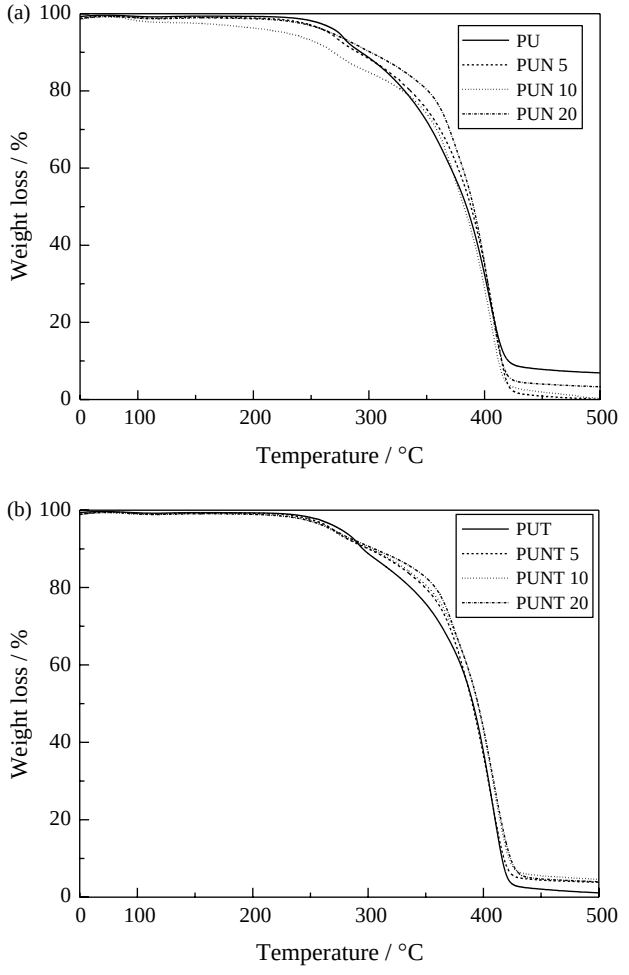

Fig. 8. TGA thermograms of PUN (a) and PUNT (b) films.

Table 3
Thermal behaviors of the films

Samples	T_i (°C)	T_{10} (°C)	T_{50} (°C)	T_{80} (°C)	T_d (°C)
PU	228	293	384	409	329
PUN5	206	289	388	409	335
PUN10	108	270	382	406	329
PUN20	228	301	390	408	350
PUT	196	301	390	410	328
PUNT5	197	302	391	410	341
PUNT10	223	304	395	414	345
PUNT20	188	305	395	415	352

suggested that NCH could lead to more physical entanglements with the PU network and contribute to their ultimate strength. Moreover, the tensile strengths of the PUNT films were significantly higher than those of PUN films. The improvement in the tensile strength could result from an enhancement in cross-linking density and strong interaction between PU and NCH molecules for the PUNT films.

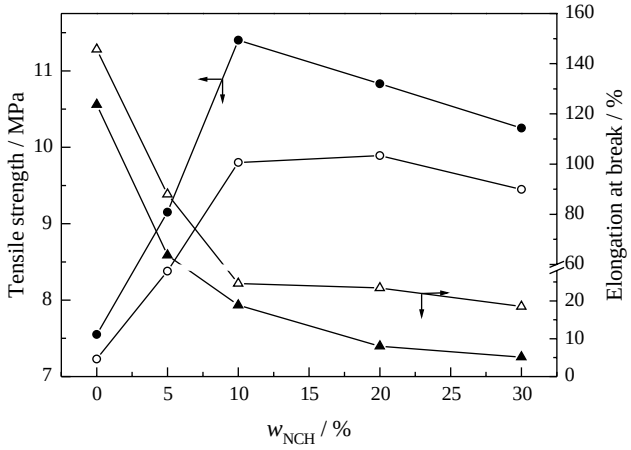

Fig. 9. NCH content (w_{NCH}) dependence of tensile strength (○, ●) and elongation at break (△, ▲) of PUN and PUNT films, respectively.

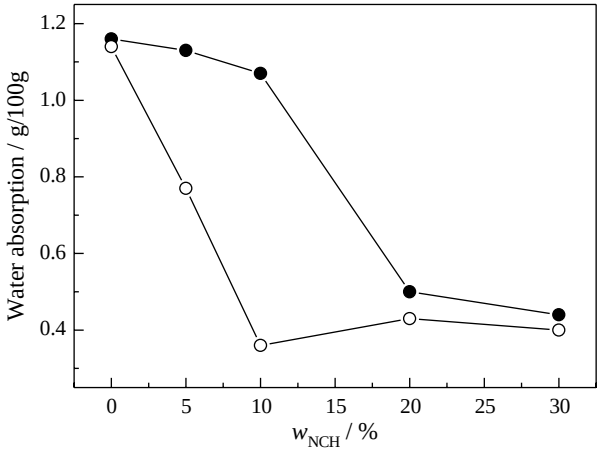

Fig. 10. The water absorption of PUN (●) and PUNT (○) films.

A solvent resistance test is a good method of determining the quality of the network density of the semi-IPN materials. Usually, as cross-linking intensity increases, the ability of the composites is able to swell in the solvent decreases. The dependence of water absorption on NCH content for the films PUN and PUNT are shown in Fig. 10. Two kinds of semi-IPN films showed negative deviation from the PU homopolymer, indicating that the semi-IPN systems can harden the solvent to swell the network structure, because of the constrained molecular chains and reduced free volume (Hsieh, Hsieh, Simon, & Tin, 1999). The PUN films absorbed more water than did PUNT films, owing to their relatively loose network structures. This revealed that water-resistance of the PUNT films was higher than that of PUN films, and increased with an increase in NCH content. The result coincided with the relatively high cross-linking density of the network structure in the PUNT films.

4. Conclusions

Two series of semi-IPN films from amorphous nitrochitosan and semicrystalline poly(ester-urethane) cross-linked by OH groups of tris(hydroxylmethyl)propane and NCO groups of PU prepolymer, respectively, were successfully prepared. They exhibited different cross-linking networks structure and properties. The PUNT films cross-linked with TMP as cross-linker had higher density, thermal stability, tensile strength and water resistance, as a result of the dense cross-linking network structure, than PUN films self-crosslinked with PU prepolymer. The results from ATR-FTIR, WAXD and DMA revealed that the degree of crystallinity of the PUNT semi-IPN system significantly decreased, compared with that of PU homopolymer. The effective interpenetration and relatively strong hydrogen bonding between PU and NCH occurred in the PUNT films cross-linked with TMP, leading to the dense network structure and a strong intermolecular interaction. Moreover, with an increase of NCH from 5 to 30 wt%, the thermal stability, tensile strength and water resistance of the PUNT films increased on the whole.

Acknowledgements

This work was supported by a major grant (59933070) from the National Natural Science Foundation of China, and the Foundation of Key Laboratory of Cellulose Chemistry, Chinese Academy of Sciences.

References

Brinkman, E., & Vandevoorde, P. (1998). Waterborne two-pack isocyanate-free systems for industrial coatings. *Progress in Organic Coatings*, *34*, 21–25.

Cascaval, C. N., Rosu, D., Rosu, L., & Ciobanu, C. (2003). Thermal degradation of semi-interpenetrating polymer networks based on polyurethane and epoxy maleate of bisphenol A. *Polymer Testing*, *22*, 45–49.

Chen, K. S., Yu, T. L., & Chen, Y. S. (2001). Soft- and hard-segment phase segregation of polyester-based polyurethane. *Journal of Polymer Research*, *8*, 99–109.

Duecoffre, V., Diener, W., Flosbach, C., & Schubert, W. (1998). Emulsifiers with high chemical resistance: A key to high performance waterborne coatings. *Progress in Organic Coatings*, *34*, 200–205.

Filip, D., Simionescu, C. I., & Macocinschi, D. (2002). Thermogravimetric analysis of liquid crystal–polymer blends. *Thermochimica Acta*, *395*, 217–223.

Gao, S., & Zhang, L. (2001). Molecular weight effects on properties of polyurethane/nitrokonjac glucomannan semiinterpenetrating polymer networks. *Macromolecules*, *34*, 2202–2207.

Hepburn, C. (1982). *Polyurethane elastomers* (p. 290). New York: Applied Science Publishers.

Howard, G. T. (2002). Biodegradation of polyurethane: A review. *International Biodeterioration & Biodegradation*, *49*, 245–252.

Hsieh, T. T., Hsieh, K. H., Simon, G. P., & Tin, C. (1999). Polymer interpenetrating polymer networks of 2-hydroxyethyl methacrylate terminated polyurethanes and polyurethanes. *Polymer*, *40*, 3153–3163.

Ikejima, T., & Inoue, Y. (2000). Crystallization behavior and environmental biodegradability of the blend films of poly(3-hydroxybutyric acid) with chitin and chitosan. *Carbohydrate Polymers*, *41*, 351–356.

Ishida, H., & Allen, D. J. (1998). Mechanical characterization of copolymers based on benzoxazine and epoxy. *Polymer*, *39*, 4487–4495.

Kuo, S. W., Chan, S. C., & Chang, F. C. (2003). Effect of hydrogen bonding strength on the microstructure and crystallization behavior of crystalline polymer blends. *Macromolecules*, *36*, 6653–6661.

Kurita, K. (2001). Controlled functionalization of the polysaccharide chitin. *Progress in Polymer Science*, *26*, 1921–1971.

Liu, H., & Zhang, L. (2001). Structure and properties of semiinterpenetrating polymer networks based on polyurethane and nitrochitosan. *Journal of Applied Polymer Science*, *82*, 3109–3117.

Lu, Y., & Zhang, L. (2002). Morphology and mechanical properties of semi-interpenetrating polymer networks from polyurethane and benzyl konjac glucomannan. *Polymer*, *43*, 3979–3986.

Luo, N., Wang, D. N., & Ying, S. K. (1996). Crystallinity and hydrogen bonding of hard segments in segmented poly(urethane urea) copolymers. *Polymer*, *37*, 3577–3583.

McKiernan, R. L., Heintz, A. M., Hsu, S. L., Atkins, E. D. T., Penelle, J., & Gido, S. P. (2002). Influence of hydrogen bonding on the crystallization behavior of semicrystalline polyurethanes. *Macromolecules*, *35*, 6970–6974.

Migashita, Y., Kobayashi, R., & Nishio, Y. (1997). Transition behavior and phase structure of chitin/poly(2-hydroxyethyl methacrylate) composites synthesized by a solution coagulation/bulk polymerization method. *Carbohydrate Polymers*, *34*, 221–228.

Muzzarelli, R. A. A. (1977). *Chitin*. New York: Pergamon Press.

Queiroz, D. P., de Pinho, M. N., & Dias, C. (2003). ATR-FTIR studies of poly(propylene oxide)/polybutadiene bi-soft segment urethane/urea membranes. *Macromolecules*, *36*, 4195–4200.

Sperling, L. H. (1981). *Interpenetrating polymer networks and related materials*. New York: Plenum Press.

Thomas, D. A., & Sperling, L. H. (1979). *Polymer blends*, Vol. 2. New York: Plenum Press.

Welsh, E. R., Schauer, C. L., Qadri, S. B., & Price, R. R. (2000). Chitosan cross-linking with a water-soluble, blocked diisocyannate. 1. Solid state. *Biomacromolecules*, *3*, 1370–1374.

Yen, F. S., & Hong, J. L. (1997). Hydrogen-bond interactions between ester and urethane linkages in small model compounds and polyurethanes. *Macromolecules*, *30*, 7927–7938.

Yen, F. S., Lin, L. L., & Hong, J. L. (1999). Hydrogen-bond interactions between urethane–urethane and urethane–ester linkages in a liquid crystalline poly(ester-urethane). *Macromolecules*, *32*, 3068–3079.

Zeng, M., Zhang, L., Wang, N., & Zhu, Z. (2003). Miscibility and properties of blend membranes of waterborne polyurethane/carboxymethylchitin. *Journal of Applied Polymer Science*, *90*, 1233–1241.

Zeng, M., Zhang, L., & Zhou, Y. (2004). Effects of solid substrate on structure and properties of casting waterborne polyurethane/carboxymethylchitin films. *Polymer*, *45*, 3535–3545.

Zhang, L., Zhou, J., Huang, J., & Gong, P. (1999). Biodegradability of regenerated cellulose films coated with polyurethane/natural polymers interpenetrating polymer networks. *Industrial and Engineering Chemistry Research*, *38*, 4284–4289.

Zhang, L., & Zhou, Q. (1999). Effects of molecular weight of nitrocellulose on structure and properties of polyurethane/nitrocellulose IPNs. *Journal of Polymer Science Part B: Polymer Physics*, *37*, 1623–1631.